

CYTOLOGICAL AND HISTOLOGICAL CHANGES
INDUCED BY WESTERN CUCUMBER MOSAIC

by

Clark Alfred Porter

A THESIS

submitted to


OREGON STATE COLLEGE

in partial fulfillment of
the requirements for the
degree of

DOCTOR OF PHILOSOPHY

June 1953

APPROVED:




Professor of Botany and Plant Pathology


In Charge of Major



Head of Department of Botany and Plant Pathology



Chairman of School Graduate Committee



Dean of Graduate School

Date thesis is presented September 22, 1952.

Typed by Colleen Hopkins

ACKNOWLEDGMENTS

The writer wishes to express his sincere appreciation to Dr. Frank P. McWhorter, Plant Pathologist, Oregon State Agricultural Experiment Station, without whose help, criticism, and inspiration this thesis would not have been possible. I am grateful to Dr. Frank H. Smith, Associate Professor of Botany, Oregon State College, for his suggestions and criticism during both the investigation and preparation of this paper. I am indebted to Mr. Clark R. Amen, Research Assistant in Entomology, Oregon State Agricultural Experiment Station, for collecting some of the plant materials used during this investigation.

TABLE OF CONTENTS

	Page
INTRODUCTION	1
MATERIALS AND METHODS	6
EXTERNAL SYMPTOMS	8
<u>Cucumis sativus</u>	8
<u>Lilium longiflorum</u> var. Croft	9
<u>Tulipa Gesneriana</u> var. Clara Butt	9
<u>Vicia faba</u>	9
OBSERVATIONS	10
<u>Cucumis sativus</u>	10
<u>Lilium longiflorum</u> var. Croft	14
<u>Tulipa Gesneriana</u> var. Clara Butt	16
<u>Vicia faba</u>	19
DISCUSSION	24
SUMMARY	27
LITERATURE CITED	30
APPENDIX (Figures 1-64 with legends)	33

CYTOLOGICAL AND HISTOLOGICAL CHANGES INDUCED BY WESTERN CUCUMBER MOSAIC

INTRODUCTION. Cellular inclusions resulting from the interaction of a virus and protoplasm are of great value in the identification of certain viruses. This is especially true in the diagnosis of animal virus diseases where inclusions have long been used as a principal means of identification (32). Unfortunately, only a comparatively few specific cellular inclusions have been demonstrated in virus infected plants. Anatomical symptoms specific for virus infections have been used in even fewer cases than inclusions for the diagnosis of plant virus diseases (21,28). Most studies dealing with virus induced anatomical changes in plants have not had as their objective the diagnosis of virus diseases. This paper deals with the anatomical symptoms produced by a virus that does not induce cell inclusions.

The present study was undertaken to determine the histological and cytological changes induced in several hosts by isolates of the cucumber mosaic virus, Marmor cucumeris Holmes, a virus of economic importance in Oregon. Isolates of M. cucumeris were selected because they produce no recognized cellular inclusions in any of their known hosts. Thus the discovery of other specific cell changes of diagnostic value would be of considerable aid. The four plant species examined were Cucumis sativus L., Lilium longiflorum Thunberg var. Croft, Tulipa Gesneriana L. var. Clara Butt, and Vicia faba L. Histological virus effects common to these very different plant species might be instrumental in the identification of the virus in other of its many hosts.

Vicia faba plants, necrotized by infection with M. cucumeris, were included in this study to determine if their necroses were similar to those of fleck in Croft Easter lily. The fleck condition is the result of infection by a virus complex (3). Marmor cucumeris in combination with the Lily Symptomless Virus, Adelonosus lilii Brierley and Smith, produces the characteristic flecking of lily leaves. The symptom produced is not a true expression of M. cucumeris alone. However, there could conceivably be specific changes attributable principally to the cucumber mosaic virus that would be of definite diagnostic value.

Most investigators agree that the yellow areas of mosaic leaves are deficient in chlorophyll and are usually thin as compared with healthy leaves (16,10,9,22,29,11,13,4). Dark green areas of mosaic-diseased leaves are often described as having elongated, narrow palisade cells that make such areas thicker than the norm (10,9,22,29,11). Investigators of other mosaic diseases report that some viruses produce little change in leaf thickness (29,31).

A common character of many mosaic diseases is the underdevelopment of yellow areas. The mesophyll of such areas is not differentiated into palisade and spongy parenchyma regions since the cells remain cuboidal and closely packed (9,22,11,13). This condition is attributed to inhibition of cell development by the virus (13,6,7). Developmental studies of mosaic-diseased plants indicate that cell divisions are suppressed in the yellow areas (9,11,6). Grainger and Heafford (14) found that certain groups of mesophyll cells in leaf primordia of mosaic-diseased tobacco became vacuolated earlier than adjacent cells and

suggested that these vacuolated cells would become the yellow areas in mature leaves. The suppression of cell division, the early vacuolation, and the precocious development of intercellular spaces in the mesophyll of yellow areas (17) indicate that these areas mature earlier than normal.

Reports in the literature vary as to whether plastid formation is inhibited or whether plastids are destroyed by mosaic viruses. Cook (6,7,5) found that the yellow areas result from inhibition of plastid formation. Since the plastids are not destroyed, the differences between the yellow and green areas may decrease with age of the leaf (6). Plastid primordia are usually destroyed in solanaceous hosts affected by aucuba mosaic (26). If plastid development is not prevented in early stages, normal development results. Other workers report degeneration of the plastids in yellow areas (4,9,11,13,16,23). Such plastids may be diffuse and irregularly shaped or, in severe cases, they fuse into amorphous masses.

Necrosis is a frequent symptom of virus-diseased plants. Sheffield (27) found for aucuba mosaic of Nicotiana glutinosa L. that during the development of local lesions, darkly staining material appeared between the cells of the lower epidermis and the spongy parenchyma. The material spread through the mesophyll and as cells were isolated they died. A few nuclear divisions occur in the mesophyll cells near the necrosis but cell division does not ensue.

Esau (12) has grouped certain virus diseases into three categories based upon the pattern of phloem degeneration produced. In the

first group of diseases, degeneration begins with sieve tube necrosis which may or may not be followed by pronounced growth disturbances. The second group includes those diseases in which phloem degeneration begins with abnormal growth and continues as a more or less extended necrosis during this growth. The diseases in the third group produce a rather generalized necrosis that affects various phloem cells and may involve other tissue.

Necrosis in Esau's third group is not specifically a phloem symptom and may originate in other tissue. In black-root disease of snap beans (18) necrosis affects various cells of the phloem, the cambium and outer vessels of xylem. Cellulose walls become covered with suberin in late phases of cellular degeneration. The necrosis in the streaked areas of the leaves of sugar cane affected with chlorotic streak (1) initiates in the mesophyll and, after the mesophyll is destroyed, spreads to the vascular bundles. Profuse gummosis occurs in mesophyll, phloem and xylem cells. Wall thickening may occur in mesophyll and epidermal cells prior to necrosis in streaked areas. Inter-cellular spherical bodies, ranging from minute dots to large spheres that nearly fill the cells, occur in bulliform cells of leaves and nodal regions of stems. When aster yellows virus induces purple-top-wilt of potato, extensive necrosis occurs in the phloem and adjacent parenchyma and, to a lesser extent, in the xylem and cambium (15,24). Cellulose and pectic walls are partially impregnated with suberin deposits in the necrotic regions of phloem and parenchyma (15).

Anatomical studies of hosts infected with M. cucumeris have been limited to cucurbits. Doolittle (10) reported that the dark green

portions of mosaic cucurbit leaves were thicker than healthy leaves, and that the yellowed areas are thinner than the green portions but of about the same thickness as healthy leaves. The palisade cells of green areas were crowded closely together and were narrower and longer than palisade cells in the healthy leaf. Palisade cells of yellowed areas were more nearly isodiametric and fewer in number per unit area than in the healthy leaf. The spongy parenchyma of the yellow areas was more compacted, and contained smaller intercellular spaces than comparable green areas. The chloroplasts in cells of yellow areas were smaller than normal and pressed closely to the cell walls.

Doolittle also noted that the conspicuous fruit symptoms were accountable to histological differences. The cells of the raised green areas and also those of the yellowed areas differed from the corresponding cells of healthy fruits. Thus, the cells beneath the epidermis of the raised green areas of diseased fruits were longer and narrower than in healthy fruits, while the cells in yellowed areas were nearly square in longitudinal section. The chloroplasts of green areas were larger and crowded more closely together than in healthy fruits.

Cook (8) reported that mosaic leaves were thinner than healthy leaves. The palisade cells in some mosaic leaves remained undeveloped and cuboidal in shape. He observed that the chlorotic cells of fruits contained noticeably fewer chloroplasts than the green cells.

MATERIALS AND METHODS. The mosaic-diseased Cucumis sativus materials used in this study were obtained from inoculated greenhouse plants and from inoculated and naturally infected field plants. The cucumber varieties used were Chicago Pickling and Snow's Perfection grown at the Oregon State College greenhouse, Snow's Perfection grown in a commercial planting near Gresham, Oregon, and in plots on the Beech farm near Corvallis, Oregon, and Lemon grown in a plot on the Oregon State College botany and plant pathology farm. Two Oregon isolates of M. cucumeris, designated as 637 and 662, were employed for inoculations. These isolates were obtained from commercial cucumber plantings in northern Oregon. The viruses responsible for the natural infections were determined by plant inoculation methods to be strains of M. cucumeris.

Lilium longiflorum var. Croft and Vicia faba plants were grown in the Oregon State College greenhouse. Materials were collected from plants exhibiting symptoms resulting from inoculation with Oregon isolate 637 of M. cucumeris.

Tulipa Gesneriana var. Clara Butt materials were collected from plants grown in a plot on the Millhollen farm near Corvallis, Oregon. These plants had been grown in the Oregon State College greenhouse the previous year and inoculated with Oregon isolate 650 of M. cucumeris. Like isolates 637 and 662, isolate 650 was obtained from a commercial cucumber planting.

Control materials were obtained from disease-free field plants, and from greenhouse plants which were either uninoculated, or inoculated

with juice from healthy plants. All control materials were collected at the same time and handled in the same manner as comparable virus-diseased materials.

The inoculation procedure employed for all plants except tulip was essentially the carborundum method described by Rawlins and Thompkins (25). Inoculations were made on the cotyledons and young leaves of cucumber plants, on the completely unfurled leaves of six-inch Vicia faba plants, and on the youngest leaves of five-inch Croft Easter lily plants. Tulips were inoculated by hypodermic injection. The hypodermic needle was inserted beneath the leaf epidermis and inoculum injected until a small water-soaked area appeared.

Materials were examined both in the living state and after sectioning in paraffin. Living materials were examined as freehand sections mounted in tap water and as whole mounts prepared by a vacuum technique (20). Randolph's modified Navashin solution (19) was employed as the killing agent for materials to be sectioned in paraffin. A modified tertiary butyl alcohol schedule (19) was used for dehydration and infiltration of all materials except mature cucumber roots and stems. These latter materials were dehydrated and cleared in amyl acetate schedule (30). All materials were embedded in paraffin of melting point range 56°-58°C. and sectioned at 5 to 25 microns. Sections were stained with several modifications of a basic hematoxylin-safranin combination (19).

EXTERNAL SYMPTOMS.

Cucumis sativus. The various symptom patterns produced in cucumber plants by M. cucumeris have been well described (10). Symptom expression, essentially the same for all varieties used, was characterized by a yellow mottling of the leaves (Fig. 1). Such mottling initiates as small yellow spots occurring irregularly over the leaf surface, which may coalesce to form large yellow areas. On other leaves the spots increase in size but remain more or less distinct, which imparts a diffuse mottle to the leaf. Green areas of mottled leaves generally do not differ in color from healthy leaves but occasional leaves exhibit dark green areas (Fig. 2). Such areas are raised, appear wrinkled, and may occur as islands surrounded by yellow tissue. All conspicuously mottled leaves are greatly reduced in size. The amount of reduction apparently depends upon the leaf size at time of infection. Terminal internodes of infected plants are shortened and also reduced in diameter. Fruit symptoms vary considerably. The most common symptom is a general reduction in green color, which results in a yellow-green fruit. Green, raised areas separated by greenish-white regions occur on some fruits and produce the appearance called "white pickle." The majority of such raised areas appear to be enlargements of the warts which normally occur beneath epidermal hairs. The raised areas are sometimes dark green in color but more often they are the same color as healthy fruits. Infected fruits are often distorted and reduced in size.

Lilium longiflorum var. Croft. The necrotic fleck condition of Croft Easter lily has been well described by Brierley and Smith (3). The flecks initiate as chlorotic areas less than 1 mm. in diameter. These areas increase in size and become elongated parallel to the leaf venation. Increase in size is accompanied by the development of brown-colored lesions that often coalesce (Figs. 3 and 4). Mature lesions, somewhat variable in size, are depressed below the leaf surface and the epidermis remains intact. The primary lesions which follow inoculation and the secondary lesions which result from systemic infection appear to develop alike.

Tulipa Gesneriana var. Clara Butt. Brierley and Doolittle (2) described the occurrence of longitudinal gray streaks on the leaves of Clara Butt tulip which appear one year after inoculation with celery and lily strains of cucumber mosaic. Somewhat similar symptoms are produced in Clara Butt tulip by M. cucumeris, Oregon isolate 650. The initial symptom is the occurrence of small gray-green areas in the leaves. These areas increase in size, become chlorotic in appearance, and later yellowish-brown in color. Large areas of an individual leaf may ultimately be affected (Fig. 5).

Vicia faba. The initial symptom of M. cucumeris, Oregon isolate 637, in V. faba is the development of brownish-black necrotic lesions at the site of inoculation (Fig. 6). The lesions, at first circular in outline and varying from 1 to 2 mm. in diameter, increase in size and become irregular in outline. The centers of the lesions become

lighter brown in color and are depressed slightly below the leaf surface. Vein necrosis results when a lesion contacts a vein. Necrosis progresses along the vein to the midrib, thence to the petiole and finally to the stem. Stem necrosis is first evident as a brownish-black streaked discoloration along one side of the stem below the infected leaf. The necrosis develops both upward and downward in the stem, but progresses downward more rapidly (Fig. 7). There is also a lateral development of necrosis which may ultimately encircle the stem.

OBSERVATIONS.

Cucumis sativus. The histological and cytological abnormalities of mosaic-diseased cucumber leaves are limited to the mesophyll of the yellow and dark green raised areas. The pathological changes in the yellow areas vary depending upon the age of the leaf at the time of virus entry. Leaves infected when young exhibit a series of pathological changes during differentiation, while leaves infected when older show only cellular modifications of a single type. The green areas of mosaic-diseased leaves do not differ histologically from healthy leaves.

In the youngest leaves in which yellow areas are discernible, premature vacuolation occurs in all mesophyll cells within these areas (Figs. 8 and 9). The development of intercellular spaces is first evident in the spongy mesophyll of the yellow areas adjacent to the lower epidermis, and may be apparent while comparable normal cells are still closely packed (Figs. 10 and 11). Thus, during the early stages of differentiation there are more intercellular spaces in the yellow areas than in comparable green areas. Also, the vacuolation of all

mesophyll cells in yellow areas is much more pronounced than in the mesophyll of healthy leaves. The individual cells of yellow areas, however, are the same size and shape as the corresponding cells of healthy leaves. As tissue differentiation continues, the development of intercellular spaces in the mesophyll of healthy leaves proceeds faster than in the mesophyll of yellow areas. This results in a reversal of the earlier difference in the amount of intercellular spaces. This difference is very apparent in mature leaves where the intercellular spaces of the palisade tissue in yellow areas are much smaller than those of comparable healthy leaves (Figs. 12 and 13). The palisade cells in healthy leaves may be 10 percent longer and 30 percent broader than those of yellow areas. However, this difference is not constant since the palisade cells in many yellow areas are indistinguishable in size from normal palisade cells.

During the early stages of development the mesophyll of yellow areas appears more mature than the mesophyll of healthy leaves. Later, at the time when the mesophyll of healthy leaves has matured, the yellow areas of infected leaves appear to be underdeveloped. This series of changes results in the mesophyll of yellow areas initially appearing hyperplastic and, later, appearing hypoplastic.

The mesophyll of the dark green raised areas exhibit abnormalities in both the palisade and spongy parenchyma regions (Figs. 14 and 15). The palisade cells of these dark green raised areas may be as much as twice the length of palisade cells in healthy leaves. The spongy parenchyma of such areas has more cells and also more intercellular

spaces than does the corresponding tissue of healthy leaves. The combination of these factors results in the dark green raised areas being thicker than healthy leaves. Thus, such areas are hyperplastic.

The nuclei occupy central positions in palisade cells and lie adjacent to walls in spongy parenchyma cells. The mesophyll cells in very young, healthy leaves are filled with plastids which are pressed so closely together that they are angular in outline (Fig. 16). As cell vacuolation and enlargement occur the plastids assume positions adjacent to the cell walls and become separated enough that they are now circular in outline (Fig. 13). This change in form is apparently due to a reduction of reciprocal pressure exerted by adjacent plastids as cell volume increases. Thus, the periphery of a mature cell is lined with circular plastids with distinct surface outlines. The chlorophyll appears to be localized in numerous granules which are embedded in a lighter colored matrix.

The plastids in yellow areas of the mesophyll in young leaves are yellow-green in color because their granules lack the definite green coloration of healthy plastids. At this early stage of differentiation the plastids are closely packed and angular in outline. In slightly older leaves, while the plastids in the mesophyll of healthy leaves of the same age are still closely packed and angular in outline, the plastids in the yellow areas assume circular shapes and are no longer closely packed. This condition prevails even though there is no difference in cell size between yellow and healthy regions and cell vacuolation in the yellow areas is much more pronounced than in

healthy leaves. The greater cell vacuolation would seem to indicate that the plastids should be more closely packed in the yellow areas than in healthy leaves. However, the plastids in the cells of the yellow areas are fewer in number and smaller in size than plastids in corresponding cells of healthy leaves (Fig. 17). These differences are not so striking in smaller cells, but become more apparent as the plastids become separated by increase in cell volume. In some cases the plastids in yellow areas lose their distinct outline and become diffuse. Such indistinct plastids coalesce to form amorphous masses. The usual condition in yellow areas is the formation of aggregates of plastids in which the individual plastids retain somewhat their distinct outlines. The plastids aggregate in the palisade cells according to two major patterns: (1) a single aggregate occurs in either the outer or inner half of a cell, partly surrounding the nucleus; a large vacuole occupies the remainder of the cell (Fig. 18); (2) aggregates occur in both ends of a cell and a third aggregate surrounds the centrally located nucleus (Fig. 19). In the latter case a vacuole is formed in each end of the cell. In spongy parenchyma cells most plastids aggregate about the nucleus adjacent to a cell wall (Fig. 20). A few plastids remain scattered in the thin layer of cytoplasm which surrounds a large central vacuole.

Plastid aggregates also develop in the mesophyll cells of yellow areas when infection occurs during intermediate stages of leaf differentiation. These aggregates are similar in appearance and placement within individual cells to the aggregates previously described. The

The later infected leaves appear not to differ histologically from healthy leaves of the same age. There are no observable differences between the amount of intercellular spaces and length of palisade cells found in the later infected leaves and comparable healthy leaves.

Lilium longiflorum var. Croft. The lesions characteristic of necrotic fleck develop in the leaves of the Easter lily as a result of mesophyll degeneration. Necrosis begins in the bundle sheath cells or in the adjacent mesophyll, and may initiate in any position about a vascular bundle (Figs. 21 and 22). The lesions are most often observed to originate centrally in the leaf and spread toward the upper and lower epidermis and in a lateral direction. All of the mesophyll about a vein will eventually become necrotic and collapse (Fig. 23); until then the cells of the vascular tissues are not visibly affected.

In young leaves developing after systemic infection the initial symptom of cellular degeneration is the aggregation of plastids about the nucleus which is located near a cell wall (Figs. 24 and 25). The plastids lose their distinct outline and coalesce into a granular mass (Fig. 26). The nucleus remains visible for a time as a distinct entity within the granular mass but soon loses its discrete appearance. All evidence of internal structure is lost and the nucleus becomes a homogeneous mass indistinguishable from the remainder of the protoplast. After the protoplast is no longer visibly granular it appears as darkly staining, coagulated deposits closely appressed to the cell wall (Fig. 27). During the disintegration of the protoplast the cell walls begin to collapse. Sometimes the walls are nearly collapsed when the

protoplast has reached its last stages of degeneration. In such cases the dark staining deposits are pressed tightly between the converging walls (Fig. 28). In other cells the contents degenerate and appear to be absorbed before the cell walls collapse.

When lesions develop in older leaves the plastids appear to degenerate in a slightly different manner. Plastids of affected cells become flattened in appearance and stain less intensely. They become vesiculated and then very diffuse in appearance (Fig. 29). Finally they lose their individuality and coalesce into a granular mass as in younger leaves.

In young leaves the epidermis is not visibly affected until after necrosis of all the mesophyll tissue in the fleck. As necrosis progresses and cells collapse, the lesion becomes a depressed area covered on both sides by normal-appearing epidermal tissue (Fig. 30). Soon occasional epidermal cells become necrotic and collapse. Eventually the entire epidermis covering a lesion may collapse but it remains as an intact cover (Fig. 31). The situation is different in older leaves where lesions appear to originate in the epidermis. In this case the first visible necrosis occurs in one to several epidermal cells (Fig. 32). Collapse of adjacent mesophyll cells in these older leaves may begin before there is much evidence of the necrotic processes described above.

As cells collapse in older leaves their contents may be in any stage of degeneration. Thus, nearly normal appearing protoplasts may appear to be pressed firmly between collapsing walls. In this case such collapsed cells contain large amounts of necrotic materials (Fig. 33).

In necrotic areas the walls of some cells may appear to be abnormally thickened. They appear very much the same as the normal thickened walls of the bundle sheath cells adjacent to the phloem which are normally thickened. These sheath cells are lignified as is shown by their staining reaction with phloroglucinol-HCl. However, close examination of the apparently thickened walls in necrotic areas shows them to be aggregations of non-lignified walls. The walls of collapsed cells become closely aligned, imparting the appearance of a single thickened wall (Fig. 34). Somewhat the same condition characterizes the process of normal phloem obliteration (Fig. 35).

Vascular tissues show no evidence of degeneration until after complete collapse of the mesophyll surrounding bundles. In such late stages of mesophyll degeneration normal appearing bundles may occur in the center of collapsed mesophyll (Fig. 23). Finally the vascular tissue also becomes necrotic and in very old lesions such tissue may be totally degenerated (Fig. 36). Vascular degeneration appears to be not a direct result of virus infection but rather an indirect effect related to association with the surrounding dead tissues.

Tulipa Gesneriana var. Clara Butt. The parenchymatous cells adjacent to bundle sheath cells in affected areas are abnormally large and their walls are considerably thickened (Figs. 37 and 38). Such walls in paraffin sections are light brown in color and appear, in this respect, the same as the walls of bundle sheath cells. The walls of both types of cells stain red with Schiff's reagent. The walls do not stain red with Sudan IV. The combination of these two reactions

indicates that the walls are lignified. Schiff's reagent is not specific for lignin since it stains cutin as well. However, when the absence of cutin in cell walls is shown by a negative Sudan IV reaction, a positive Schiff's test indicates the presence of lignin. The enlargement of cells and thickening of cell walls is accompanied by crushing of some bundle sheath and parenchymatous cells (Figs. 39 and 40). Cell collapse is preceded by the development of thickened walls and degeneration of the protoplast.

The contents of collapsing cells appear as heavily stained coagulated masses. Complete collapse of several adjacent cells results in the occurrence of wall aggregates interspersed with darkly staining protoplasts (Fig. 41). During the early stages of symptom development the necrotic contents of collapsed cells appear to be largely absorbed. Cells affected in later development exhibit coagulated contents before there is evidence of collapse.

Cell collapse results in the formation of large voids within the mesophyll (Fig. 42). These voids have their greatest dimension in a plane parallel to the long axis of the associated bundle. They may extend from the upper to the lower epidermis as seen in a cross section of the leaf. Aggregated walls of collapsed cells form the boundaries between voids and the surrounding tissues. Coagulated cell contents may often be closely appressed to the void side of this boundary.

Vascular tissues are initially unaffected. In advance stages of mesophyll degeneration bundles may show signs of necrosis (Fig. 43).

This condition does not prevail until the sheath is crushed and the surrounding mesophyll collapsed. Often, normal-appearing bundles are surrounded by crushed sheath cells and nearly encircled by voids. The only supports furnished such bundles are narrow ridges of collapsed cells extending to the upper and lower epidermis.

Rarely does the epidermis show signs of degeneration. Small areas of epidermis may collapse over mesophyll that is in very late stages of degeneration. More often, the epidermis remains intact and turgid even in those areas where a void in the mesophyll occurs immediately beneath the epidermis (Fig. 41). For this reason, the affected areas of leaves are not depressed below the surface. The epidermis over such areas remains intact and maintains its normal position relative to the epidermis covering unaffected areas.

After the initial enlargement of cells and the thickening of their walls, degeneration is evidenced by large deposits of necrotic material within uncollapsed cells. It appears that the protoplast dies before collapse occurs, while in the Easter lily death of the protoplast and collapse of the cells occurs almost simultaneously.

Suitable materials were not available for a complete study of cellular degeneration. The effects, however, are first evident in the plastids and cytoplasm. The plastids of affected cells are often vesiculate and the cytoplasm is coagulated (Fig. 44). The nucleus remains discernible longer than other cell constituents but it eventually disintegrates and becomes indistinguishable in the mass of necrotic protoplasmic material.

Vicia faba. The lesions in V. faba leaves induced by inoculation with M. cucumeris initiate in the palisade tissue of the mesophyll. The protoplasts necrose and form deposits of darkly stained material confined within individual cells. The walls of such cells soon collapse. Cellular degeneration progresses downward and laterally through the mesophyll (Figs. 45 and 46). The necroses are equally apparent in the palisade and spongy mesophyll regions but decrease in severity laterally from the center toward the periphery of the lesions.

Cellular degeneration in the mesophyll is first evident in the plastids which become granular in appearance and tend to aggregate about the nucleus (Figs. 47 and 48). They soon become diffuse in appearance and sometimes become vesiculate (Fig. 49). At this time the dense cytoplasm becomes granular throughout. The plastids coalesce into finely granular masses which become indistinguishable from the cytoplasm (Fig. 50). The nucleus loses its normal appearance, and becomes a darkly staining amorphous mass. The final stage in cellular degeneration is the collapse of the cell walls. Thus, the fully developed lesion consists of masses of necrotic protoplasmic material with collapsed cell walls dispersed throughout (Fig. 45).

Degeneration of epidermal cells proceeds in a similar manner but does not occur until after necrosis of the mesophyll beneath. The protoplasts of epidermal cells necrose but their walls collapse only over the central and most severely necrotic portion of the mesophyll. The radial, transverse, and inner tangential walls collapse but the outer tangential walls remain intact and stain heavily with

safranin and hematoxylin. The collapse of cell walls results in a slight depression of the epidermis over the central portion of the lesion (Fig. 45).

The sheath cells of vascular bundles necrose following degeneration of nearby mesophyll. The initial effects may occur in any portion of the sheath but most often originate in the region adjacent to the xylem (Fig. 51).

Changes in xylem vessel walls are evident in areas where the surrounding bundle sheath and mesophyll are necrotic. The walls of such vessels are stained much darker than those of normal vessels. This dark staining effect is first evident at the corners of the vessels, subsequently extending around the entire wall as seen in transverse section. Simultaneously with changes in vessel walls, other cells within the bundle become necrotic until degeneration is general throughout the bundle.

An exudate is present in xylem vessels of those veins having necrotic sheath cells (Fig. 51). The staining reaction of the exudate with phloroglucinol-HCl varies from reddish-yellow to very dark red; thus indicating the exudate is wound gum in various stages of formation.

Necrosis in the young stem is at first restricted to the phloem of a single vascular bundle, the pericycle parenchyma, and immature pericycle fibers (Figs. 52 and 53). The longitudinal progression of the necrosis through the stem is most rapid in or near the initially necrotic bundle. Later, the necrosis becomes rather general and

involves also the cortex, cambium, xylem, and pith (Fig. 54). At a given level, the necrosis initially spreads from a necrotic bundle to adjacent bundles through the parenchyma of the pericycle, cortex, or pith. Necrosis also progresses longitudinally through various tissues other than those in or about the initially necrotic bundle. This longitudinal spread lags behind that through the initially necrotic bundle.

In early stages of necrosis of the pericycle parenchyma cells the cytoplasm becomes granular in appearance. It soon forms deposits that line the cell walls, stain deeply, and often impart a thickened appearance to the walls. The walls collapse and the necrosed tissue appears as masses of darkly stained protoplasmic material interspersed with cell walls (Fig. 55). Such masses are brownish-yellow in fresh sections and stain reddish-yellow with phloroglucinol-HCl. The most severe necrosis occurs in those cells between the phloem and pericycle fibers opposite each vascular bundle. As necrosis progresses, the collapse of cells extends around the periphery of the phloem to the interfascicular cambium (Fig. 56).

The first degenerative changes apparent in immature pericycle fibers is the distortion of cell walls (Fig. 55). The protoplasts necrose and stain dark red with safranin. The fibers eventually collapse completely and the entire mass of degenerated fibers becomes continuous with the already necrotic pericycle parenchyma (Fig. 57).

Cortical parenchyma and fibers necrose in the same manner as the corresponding pericycle cells but generally do not become

affected until the necrosis is rather general throughout adjacent vascular tissue (Fig. 57).

Necrosis of the phloem involves sieve tubes, companion cells and parenchyma. In early stages, companion cells are the most extensively destroyed but initial necrosis is not restricted to them. Any area within the phloem may show first effects, the necrosis becoming apparent simultaneously with that in the pericycle parenchyma (Fig. 58). The protoplasts of individual cells degenerate into darkly staining amorphous masses and the cell walls are also affected. When several adjacent cells necrose, the result is a deposit of darkly staining material within which cell walls form irregular patterns (Fig. 59).

Both interfascicular and fascicular cambium may become necrotic. Isolated areas of interfascicular cambium may necrose or the necrosis may be continuous with that of the pericycle parenchyma (Fig. 56). Necrosis is usually restricted to tiers of cells wherein two or three primarily necrosed cells are apparent. The protoplasts become granular and degenerate into irregular masses within individual cells. Necrosis of fascicular cambium is apparent only in those regions where vascular tissues are severely necrotic, and is continuous with the degenerated vascular tissue (Fig. 60). Large areas may be affected and form darkly staining masses which appear the same as those formed in necrotic phloem.

The first effect exhibited by the xylem is the deposition of wound gum in the vessels. Vessels may contain gum even though necrosis is not apparent in or about the bundle. The gum appears finely

granular at first, and stains light brownish-red with phloroglucinol-HCl. Later the deposits become homogeneous and stain very dark red with the same reagent (Fig. 61). Necrosis of xylem parenchyma is first evidenced by protoplast degeneration followed by collapse of walls. In general, xylem necrosis is most severe near the cambium and decreases in severity deeper within the tissue (Fig. 60). However, necrosis may make its first appearance in a bundle in the primary xylem as a result of spread through pith parenchyma from a necrotic bundle (Fig. 62). In such cases the primary xylem is the only portion of the bundle exhibiting necrosis and this occurs only in those regions of the stem where there are other bundles which are severely necrotic. In the most severe stages of necrosis the walls of vessels and parenchyma stain darker with safranin.

In regions of the stem where necrosis is most severe, degeneration of pith parenchyma is apparent (Fig. 54). Such degeneration is usually in areas adjacent to the severely necrotic bundles, but may extend through the parenchyma to other bundles. Eventually the parenchyma cells of the pith collapse, forming necrotic masses like those described as occurring in pericycle parenchyma. Isolated areas of necrotic pith parenchyma may be seen when the stem is viewed in cross section (Fig. 63). Such necrotic areas result from the longitudinal spread of necrosis through the pith.

Spherical bodies ranging in size from less than 1 micron to 6 microns are present in phloem, cambium, xylem parenchyma, and pericycle parenchyma cells of severely necrotic stems (Fig. 64). Aggregates

of bodies of intermediate size are usually found in cells adjacent to severely necrosed cells. These occur most abundantly in the phloem and to a lesser extent in pericycle parenchyma. The individual bodies within an aggregate may be somewhat ovoid. The smaller bodies occur at greater distances from obvious necroses and usually appear to line the inner walls of phloem, cambium, and xylem parenchyma cells. Occasionally, large spheres are present in cells but they are not as general in occurrence as the intermediate and small-sized bodies. Nuclei may be present within the same cells where the various bodies occur. All of the bodies are colorless in unstained sections, stain light to bright pink with safranin, do not stain with Sudan IV, and are not optically active in polarized light. These observations show that the spheres do not possess crystalline structures, and that they apparently contain no fatty materials.

DISCUSSION. In general, the results of the present study of mosaic-diseased cucumber leaves agree with the studies of other mosaic diseases (4,9,10,11,13,16,22,29). The histological and cytological abnormalities of leaves are restricted to the mesophyll of the yellow and the dark green raised areas. The yellow areas in young leaves appear hyperplastic because they exhibit certain characteristics of older, healthy leaves. This early differentiation in yellow areas is attributable to the suppression of cell divisions, the premature cell vacuolation, and the early development of intercellular spaces. The yellow areas in old leaves appear hypoplastic because they do not complete the typical mesophyll differentiation of healthy leaves. The

yellow areas have less intercellular spaces than normal and the palisade cells may be slightly shortened. However, the palisade cells of yellow areas are usually the same size as those of comparable healthy leaves. Some mosaic diseases inhibit the differentiation of mesophyll into palisade and spongy parenchyma tissues (9,11,13,22) and all cells remaining cuboidal and closely packed. This is not the case in mosaic-diseased cucumber leaves where development of distinct palisade and spongy parenchyma regions occur. This variation, as well as others, is understandable. Viruses differ in virulence, and the age of the leaf at the time of infection influences the severity of symptoms produced. Goldstein (13) has shown that leaves infected when young exhibit more marked internal abnormalities than leaves infected when they were partly differentiated. The results of the present study on mosaic-diseased cucumber leaves are in agreement with Goldstein's conclusions. Environmental factors may also influence symptom expression. This is shown by the intensification or reduction of symptom severity that results when mosaic-diseased plants are subjected to certain conditions of light, temperature, or nutrition.

The mesophyll in dark green areas of mosaic-diseased cucumber leaves appears to be hyperplastic. This is in agreement with Doolittle's findings concerning such areas (10). When compared with the mesophyll of healthy leaves, the palisade cells of dark-green raised areas are decidedly longer, and there is more spongy parenchyma with a greater amount of intercellular spaces. Thus, the dark green areas are thicker than comparable areas of healthy leaves.

These studies indicate that both inhibition of development and destruction of plastids occur in the yellow areas. Inhibition results in the plastids being reduced in number and size. Some plastids appear to develop normally for a time and then form aggregates. These aggregates may be formed in leaves during both the early and intermediate stages of differentiation. This may be the initial stage in plastid degeneration since it seems that such plastids do not recover. This conclusion appears to be substantiated by the fact that the plastids in yellow areas of mosaic-diseased cucumber leaves have never been observed to return to a normal condition as has been reported to occur in mosaic-diseased sugar cane, canna, and tomato (6). Some plastids in yellow areas of cucumber leaves become diffuse and coalesce into amorphous masses. Plastid abnormalities similar to those observed in the present study have been described by other workers. Dickson (9) mentions agglomerations of chloroplasts and their coalescence into irregular green masses in the yellow areas of mosaic-diseased tobacco and potato plants. In a description of bean mosaic, Nelson (23) states that chloroplasts become flattened and collapse into a coherent mass of pale-yellow or colorless material. The vesiculation and coalescence of chloroplasts may be induced by agents other than viruses (11,33,34). Esau (11) does not regard plastid changes in mosaic plants as responses to any specific action of the viruses.

The necrotic symptoms of Easter lily, tulip, and V. faba, produced by M. cucumeris, originate in the mesophyll of leaves. The necrosis in Easter lily and tulip is restricted primarily to this

tissue, and invades vascular tissue only during the late stages of mesophyll degeneration. Contrary to this, the necrosis of leaves and stems of V. faba rapidly becomes general.

The necrosis in tulip is accompanied by growth abnormalities in the mesophyll. There is an enlargement of cells and a thickening of cell walls in advance of obvious necrosis. A similar thickened-wall condition has been reported as occurring in the chlorotic streak of sugar cane (1). The necrosis of Easter lily and V. faba results in cell collapse but there are no associated growth abnormalities. Spherical inclusions, somewhat similar to those found in V. faba, are reported to occur in sugar cane chlorotic streak (1).

Whether or not the necroses in the plants examined are specific symptoms that can be used for diagnosis must await further investigations of the symptoms produced by other viruses in these same hosts. One such investigation was made prior to this study. Lily rosette was found to produce phloem necrosis in Easter lily (21). This is quite different from the mesophyll degeneration produced in Easter lily by M. cucumeris. It is such differences that render anatomical symptoms useful for diagnosis of virus diseases.

SUMMARY. The effects of Marmor cucumeris, the cucumber mosaic virus, on the cytology and histology of cucumber, Easter lily, tulip, and V. faba were studied.

Marmor cucumeris produces a mottle symptom in cucumber, and necrotic symptoms in Easter lily, tulip, and V. faba.

Yellow areas in young cucumber leaves appear hyperplastic because of the suppression of cell division, premature vacuolation, and the early development of intercellular spaces. As the leaf matures these same areas appear hypoplastic because there are less intercellular spaces than in healthy leaves and palisade cells are sometimes shortened. Yellow areas in leaves infected during intermediate stages of differentiation appear not to differ histologically from comparable healthy leaves.

The plastids in yellow areas of mottled cucumber leaves are both inhibited in development, and destroyed. Inhibition results in the plastids being reduced in number and size. Some plastids in yellow areas become diffuse and coalesce into amorphous masses. Plastid aggregates may form in the cells of yellow areas in leaves that were infected during early differentiation and, also in leaves infected during later differentiation.

The necrosis in tulip leaves is restricted largely to the mesophyll and is accompanied by cell enlargement and cell wall thickening. Large voids develop in necrotic areas as the result of cell collapse.

Necrosis in Easter lily is restricted primarily to the mesophyll of leaves and does not progress to the epidermal and vascular tissues until the mesophyll is degenerated. Cells in necrotic areas collapse but there are no associated growth abnormalities.

Necrosis in V. faba leaves initiates in the mesophyll and spreads rapidly to the epidermal and vascular tissues. The necrosis in the

stem is at first restricted to the phloem of a single vascular bundle and the adjacent pericycle. The necrosis soon becomes general throughout the cortex, pericycle, phloem, cambium, xylem, and pith. Non-crystalline spherical inclusions occur in the cells that are adjacent to severely necrotic areas.

LITERATURE CITED

1. Abbott, E. V. and J. E. Sass. Pathological histology of sugar cane affected with chlorotic streak. Jour. Agr. Res. 70:201-207. 1945.
2. Brierley, P. and S. P. Doolittle. Some effects of strains of cucumber virus 1 in lily and tulip. Phytopath. 30:171-174. 1940.
3. Brierley, P. and F. F. Smith. Studies on lily virus diseases: the necrotic-fleck complex in Lilium longiflorum. Phytopath. 34:529-555. 1944.
4. Clinch, P. Cytological studies of potato affected with certain virus diseases. Roy. Dublin Soc. Sci. Proc. 20:143-172. 1932.
5. Cook, M. T. Histology and cytology of sugar cane mosaic. Jour. Dept. Agr. Porto Rico 9:5-27. 1925.
6. ——— The effect of some mosaic diseases on cell structure and on the chloroplasts. Porto Rico Dept. Agr. Jour. 14:69-101. 1930.
7. ——— The effect of mosaic on cell structure and chloroplasts. Jour. Dept. Agr. Porto Rico 15:177-181. 1931.
8. ——— Cucumber mosaic in Puerto Rico. Jour. Agr. Univ. Puerto Rico 22:443-447. 1938.
9. Dickson, B. T. Studies concerning mosaic diseases. Macdonald Col. McGill Univ. Tech. Bull. 2:1-125. 1922.
10. Doolittle, S. P. The mosaic disease of cucurbits. U.S.D.A. Bull. No. 879. Nov. 15, 1920. 69p.
11. Esau, K. Anatomical and cytological studies on beet mosaic. Jour. Agr. Res. 69:95-117. 1944.
12. ——— Some anatomical aspects of plant virus disease problems II. Bot. Review 14:413-449. 1948.
13. Goldstein, B. A cytological study of the leaves and growing points of healthy and mosaic diseased tobacco plants. Torrey Bot. Club Bull. 53:499-599. 1926.

14. Grainger, J. and R. M. Heafford. Some effects of the ordinary tobacco mosaic upon the developmental anatomy of the host plant. Leeds Phil. and Lit. Soc. Proc. 2:406-415. 1933.
15. Hill, L. M. and C. R. Orton. Microchemical studies of potato tubers affected with blue stem disease. Jour. Agr. Res. 57:387-392. 1938.
16. Hoggan, I. A. Cytological studies on virus diseases of solanaceous plants. Jour. Agr. Res. 53:651-671. 1927.
17. Iwanowski, D. ^{II}Über die Mosaikkrankheit der Tobakspflanze. Ztschr. f. Pflanzenkrankh. 13:1-41. 1903.
18. Jenkins, W. A. A histological study of snap bean tissues affected with black root. Jour. Agr. Res. 62:683-690. 1941.
19. Johansen, D. A. Plant microtechnique. New York, McGraw-Hill, 1940. 523p.
20. McWhorter, F. P. The examination of tissues in living leaves and flowers by means of a high vacuum technic. Stain Tech. 26:177-180. 1951.
21. _____ and P. Brierley. Anatomical symptoms useful in diagnosis of lily rosette. Phytopath. 61:66-71. 1951.
22. Matsumoto, T. Some experiments with azuki-bean mosaic. Phytopath. 12:295-297. 1922.
23. Nelson, R. Investigations in the mosaic disease of bean (Phaseolus vulgaris L.). Mich. Agr. Expt. Sta. Tech. Bull. 118. 71p.
24. Orton, C. R. and L. M. Hill. An undescribed potato disease in West Virginia. Jour. Agr. Res. 55:153-157. 1937.
25. Rawlins, T. E. and C. M. Tompkins. Studies on the effect of carborundum as an abrasive in plant virus infections. Phytopath. 26:578-587. 1936.
26. Sheffield, F. M. L. The development of assimilatory tissue in solanaceous hosts infected with aucuba mosaic of tomato. Ann. Appl. Biol. 20:57-69. 1933.
27. _____ The histology of the necrotic lesions induced by virus diseases. Ann. Appl. Biol. 23:752-758. 1936.

28. _____ Value of phloem necrosis in the diagnosis of potato leaf-roll. Ann. Appl. Biol. 30:131-136. 1943.
29. Smith, F. F. Some cytological and physiological studies of mosaic diseases and leaf variegations. Mo. Bot. Gard. Ann. 13:425-484. 1926.
30. Smith, F. H. Amyl acetate as a clearing agent for refractory plant materials. Stain Tech. 26:271-272. 1951.
31. Stone, W. E. Effects of some mild forms of mosaic on potato and a few other plants. Jour. Agr. Res. 65:195-207. 1942.
32. van Rooyen, C. E. and A. J. Rhodes. Virus diseases of man. New York, Thomas Nelson and Son, 1948. 1202p.
33. Weir, T. E. Neutral red staining in the protonema of Polytrichum commune. Amer. Jour. Bot. 23:645-652. 1936.
34. _____ The structure of the chloroplast. Bot. Rev. 4:497-530. 1938.

APPENDIX

Figures 1 through 64 with legends.

Figures 1, 2, 3, 4 and 5 courtesy of Dr. F. P. McWhorter.

Photomicrographs of leaves (Figs. 8-51) and stems (Figs. 52-64) are of transverse sections.

Cucumber mosaic virus is designated by CMV.

Fig. 1. Cucumber leaves. CMV. Mottle patterns.

Fig. 2. Cucumber leaf. CMV. Dark green raised areas and yellow patching.

Fig. 3. Easter lily. CMV. Necrotic flecks on leaves.

Left: severe flecking with some distortion.

Center: mild flecking.

Right: severe flecking and chlorosis.

Fig. 4. Easter lily. CMV. Front: mature flecks on leaves, twisting of leaves, and general stunting. Back: healthy control.

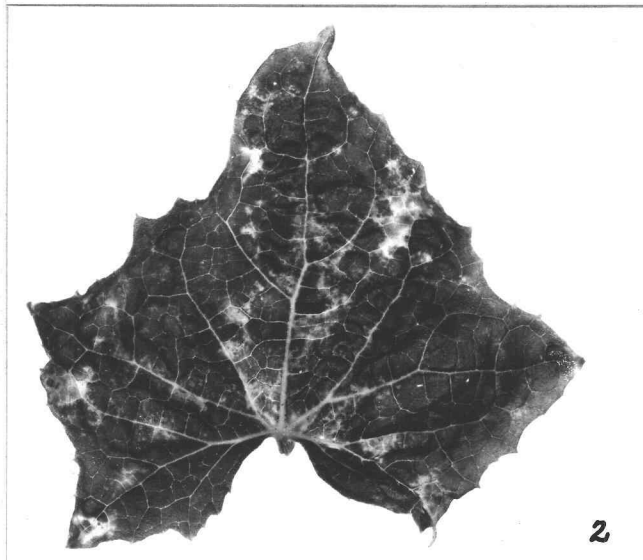
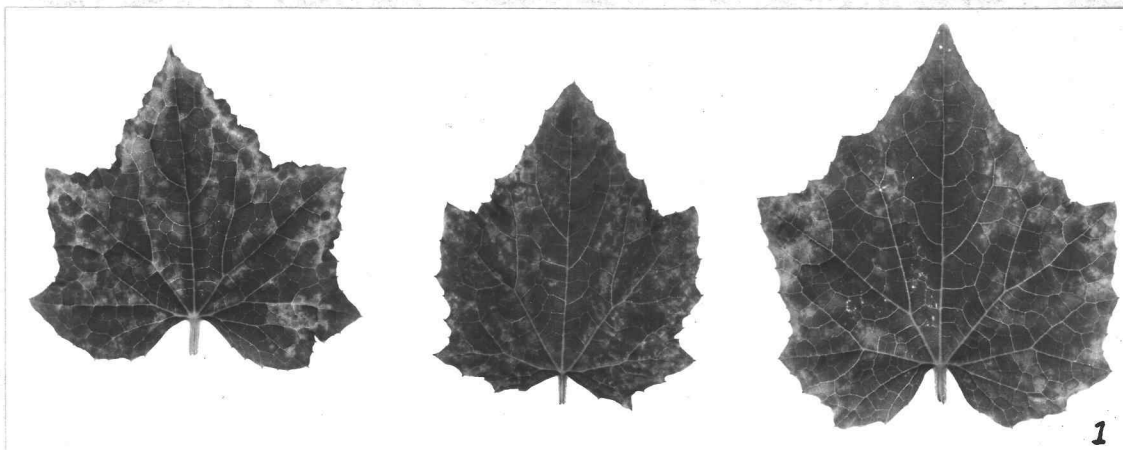


Fig. 5. Tulip. CMV. Left: severe leaf symptom; large chlorotic areas. Right: initial symptom; small gray-green areas.

Fig. 6. Vicia faba. CMV. Brownish-black necrotic lesions on inoculated leaf.

Fig. 7. Vicia faba. CMV. Lower: brownish-black discoloration of stem resulting from necrosis. Upper: healthy stem.

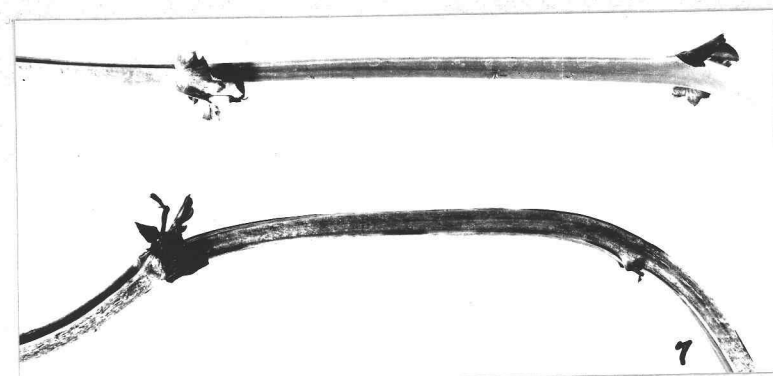
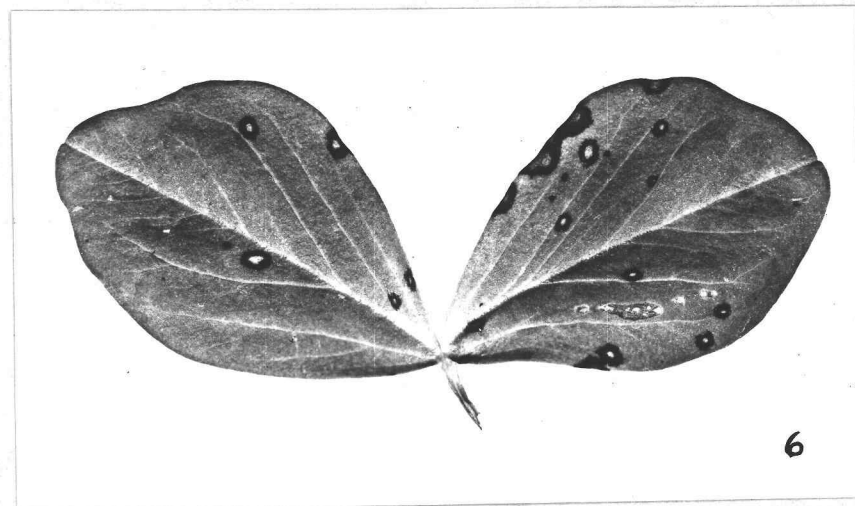


Fig. 8. Cucumber leaf. CMV. Premature vacuolation of mesophyll in yellow area. 400x.

Fig. 9. Cucumber. Healthy leaf same age as Fig. 8. 400x.

Fig. 10. Cucumber leaf. CMV. Early development of intercellular spaces in spongy parenchyma of yellow area. 400x.

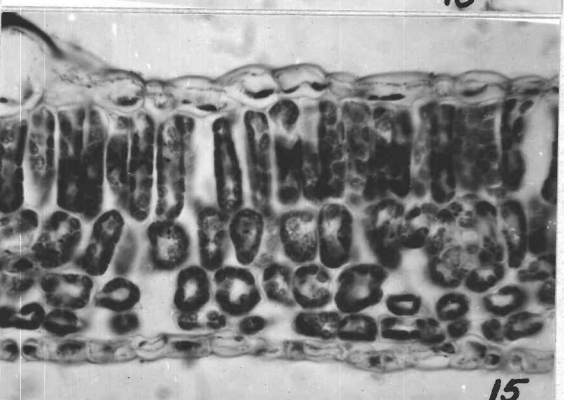
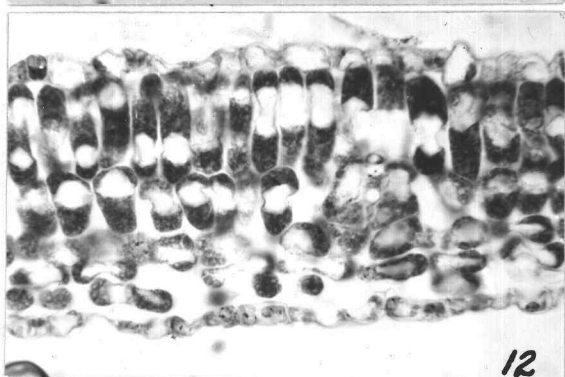
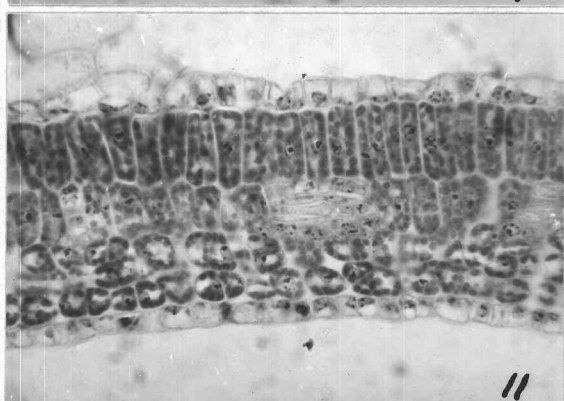
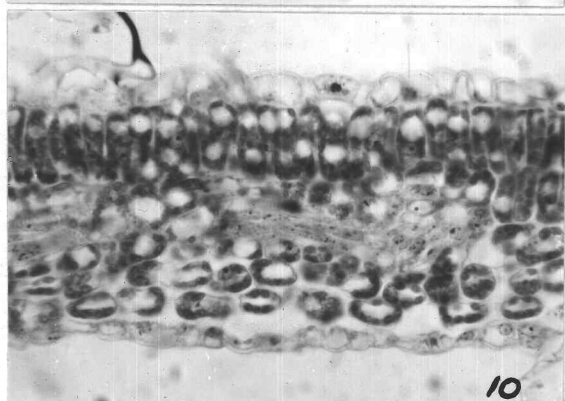
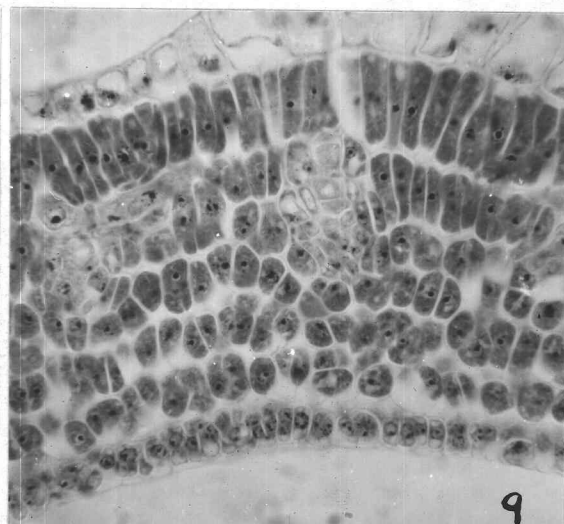
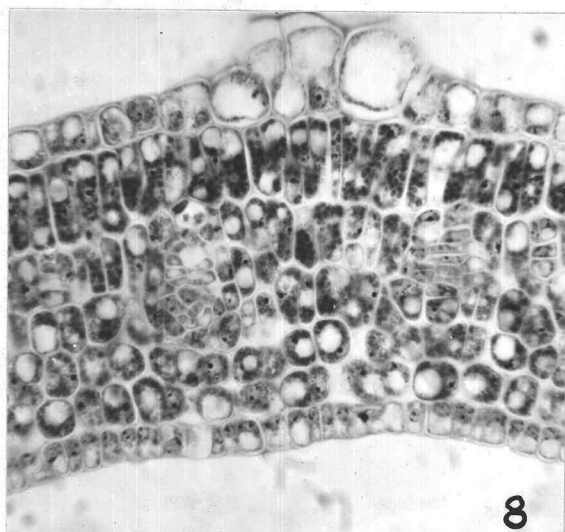
Fig. 11. Cucumber. Healthy leaf same age as Fig. 10. 400x.

Fig. 12. Cucumber leaf. CMV. Closely packed palisade cells of yellow area. 400x.

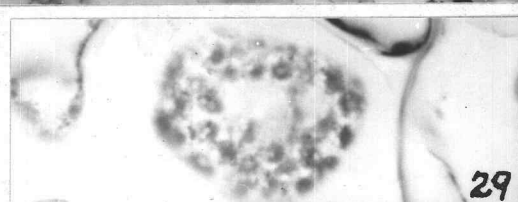
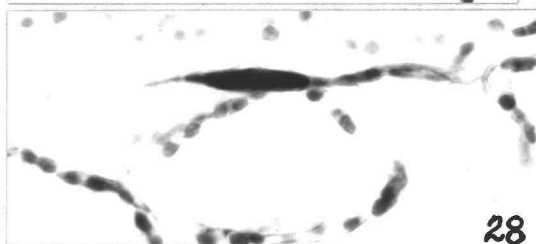
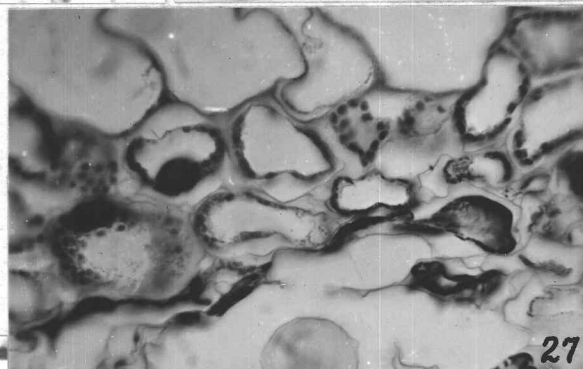
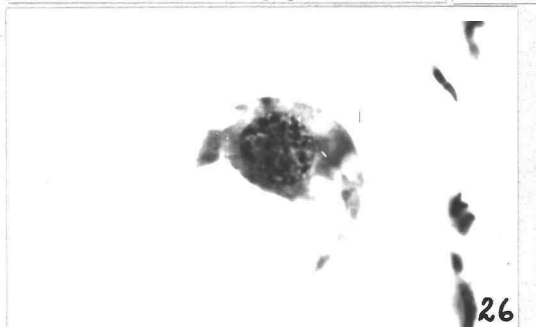
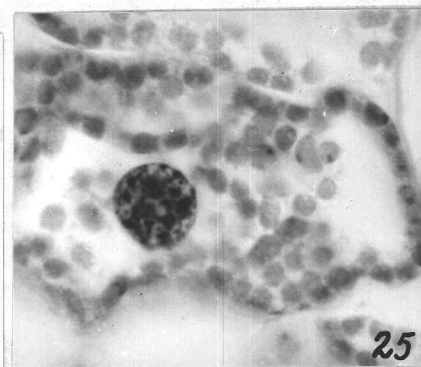
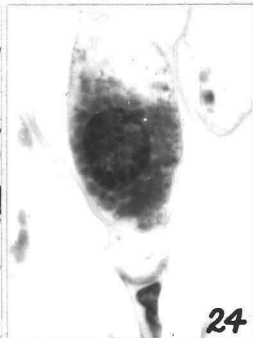
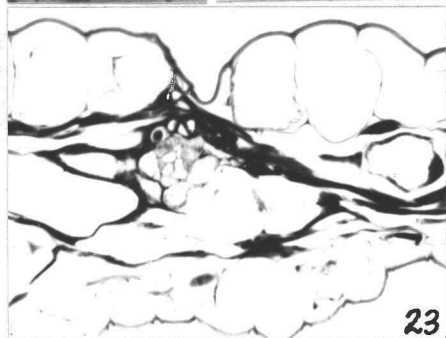
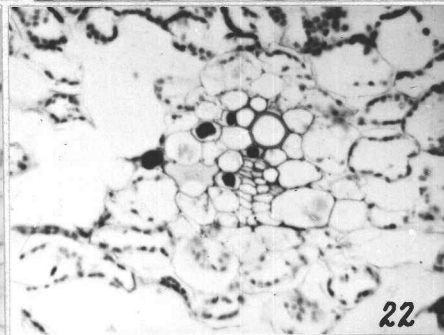
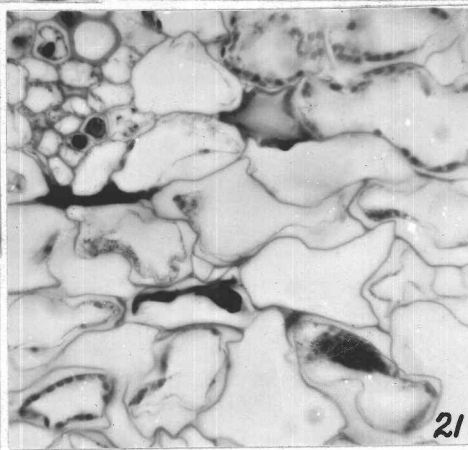
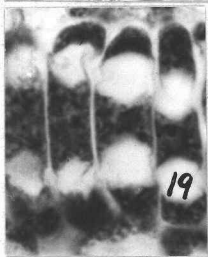
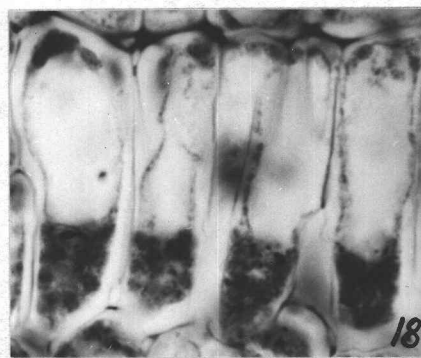
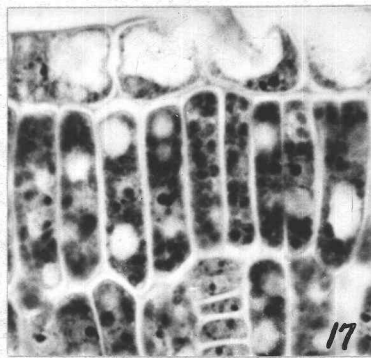
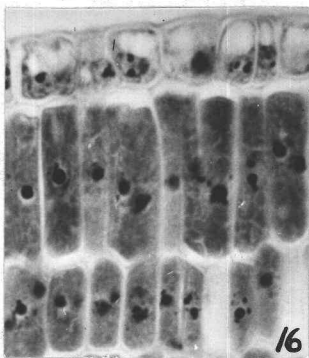
Fig. 13. Cucumber. Healthy leaf same age as Fig. 12. Plastids are adjacent to cell walls and circular in outline. 400x.

Fig. 14. Cucumber leaf. CMV. Dark green raised area exhibiting abnormally long palisade cells (left), and spongy parenchyma with increased number of cells and intercellular spaces. 400x.

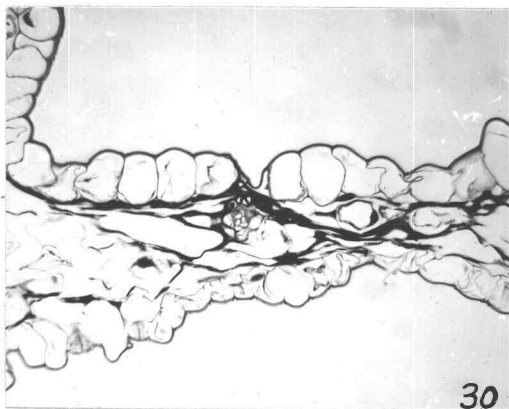
Fig. 15. Cucumber. Healthy leaf same age as Fig. 14.



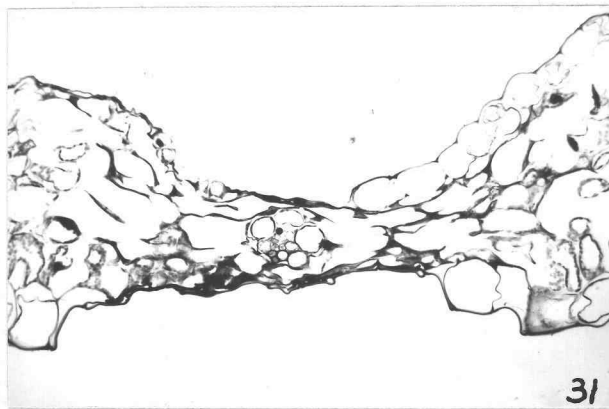
- Fig. 16. Cucumber. Healthy leaf. Mesophyll cells filled with closely packed angular plastids. 800x.
- Fig. 17. Cucumber leaf. CMV. Plastids in yellow area reduced in number and size. 800x.
- Fig. 18. Cucumber leaf. CMV. Plastids aggregated about nucleus in lower half of palisade cells in yellow area. 800x.
- Fig. 19. Cucumber leaf. CMV. Plastids aggregated in both ends and about centrally located nucleus of palisade cells in yellow area. 800x.
- Fig. 20. Cucumber leaf. CMV. Plastids aggregated about nucleus adjacent to cell wall in spongy parenchyma. 800x.
- Fig. 21. Easter lily leaf. CMV. Necrosis initiating in the bundle sheath and adjacent mesophyll. 400x.
- Fig. 22. Easter lily. Healthy leaf same age as Fig. 21. 200x.
- Fig. 23. Easter lily leaf. CMV. Necrosis and collapse of mesophyll about a normal appearing vein. 200x.
- Fig. 24. Easter lily leaf. CMV. Cellular degeneration beginning with aggregation of plastids about nucleus of mesophyll cell. 800x.
- Fig. 25. Easter lily. Healthy leaf. Mesophyll cell from leaf same age as Fig. 24. 800x.
- Fig. 26. Easter lily leaf. CMV. Plastids of mesophyll cell have lost their distinct outlines and coalesced into a finely granular mass. 800x.
- Fig. 27. Easter lily leaf. CMV. Darkly staining necrotic protoplasts of mesophyll cells. 400x.
- Fig. 28. Easter lily leaf. CMV. Darkly staining protoplast of necrotic mesophyll cell appressed between converging walls. 800x.
- Fig. 29. Easter lily leaf. CMV. Vesiculated plastids in mesophyll cell of older leaf. 800x.



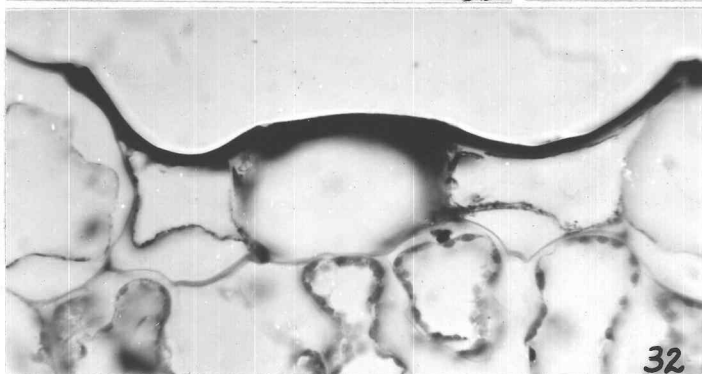
- Fig. 30. Easter lily leaf. CMV. Necrotic area covered by normal appearing epidermal tissue. 100x.
- Fig. 31. Easter lily leaf. CMV. Collapsed epidermal tissue forming intact cover over lesion. 100x.
- Fig. 32. Easter lily leaf. CMV. Initiation of necrosis in epidermal cells. 400x.
- Fig. 33. Easter lily leaf. CMV. Deposits of necrotic material resulting from cell collapse. 400x.
- Fig. 34. Easter lily leaf. CMV. Cell wall aggregate appearing as a single thickened wall. 800x.
- Fig. 35. Easter lily. Healthy leaf. Cellular degeneration resulting from phloem obliteration (bottom). 800x.
- Fig. 36. Easter lily leaf. CMV. Necrosis of vascular bundle following collapse of surrounding mesophyll. 400x.
- Fig. 37. Tulip leaf. CMV. Enlarged parenchymatous cells with thickened walls adjacent to bundle sheath. 100x.
- Fig. 38. Tulip. Healthy leaf same age as Fig. 37. 100x.



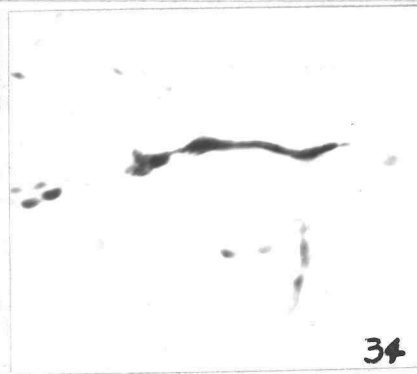
30



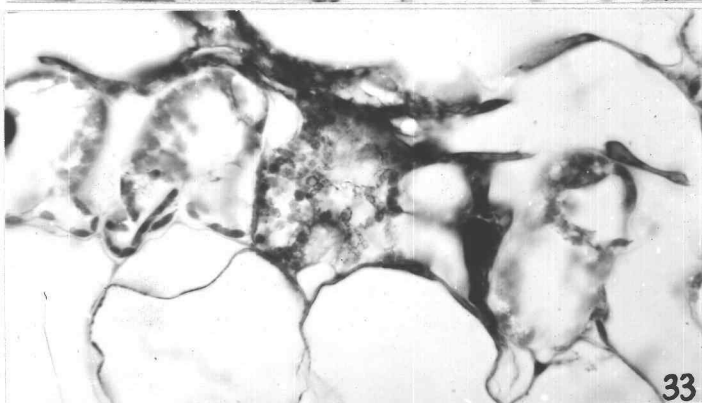
31



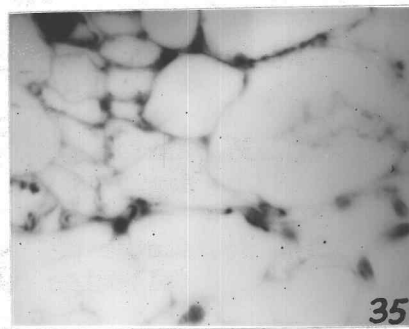
32



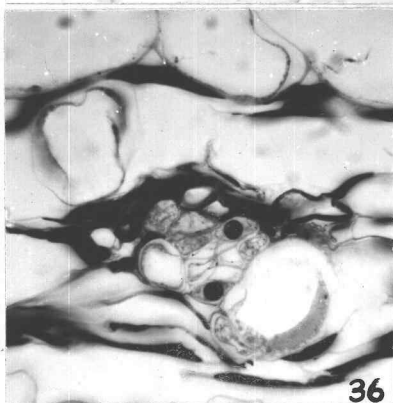
34



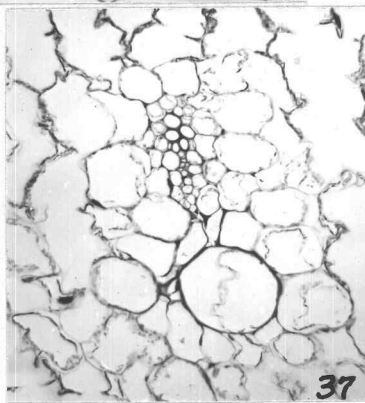
33



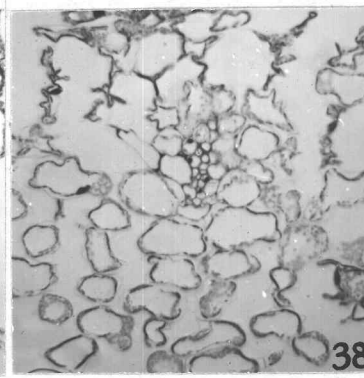
35



36

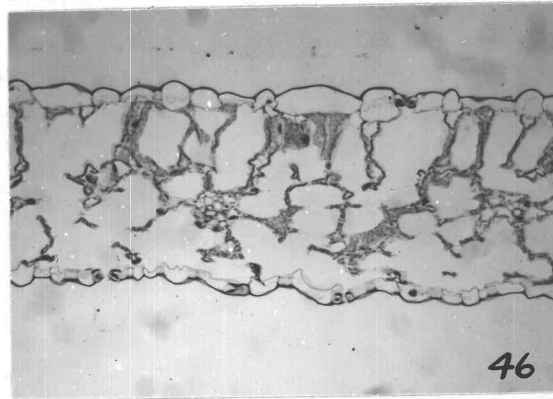
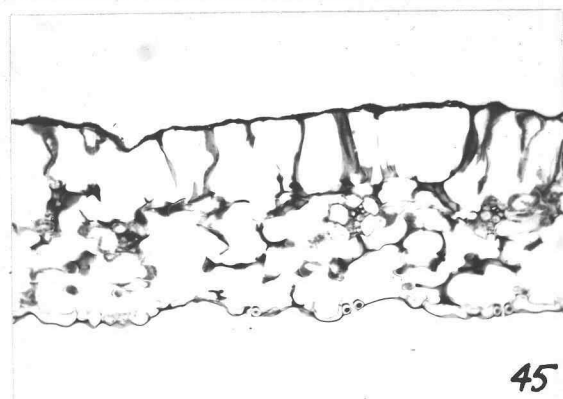
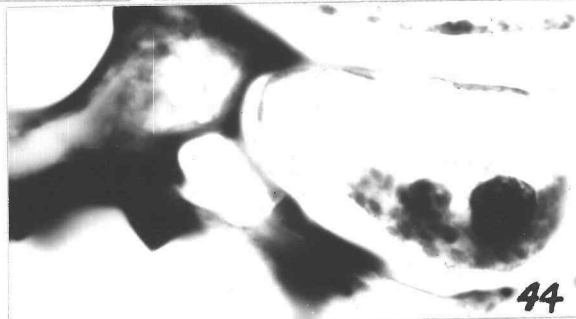
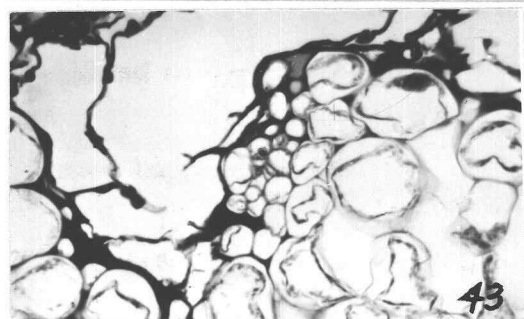
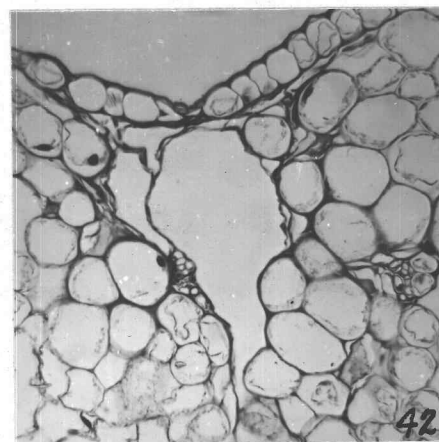
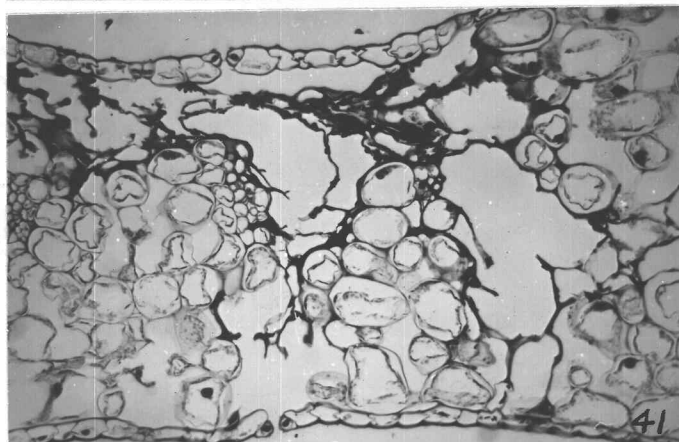
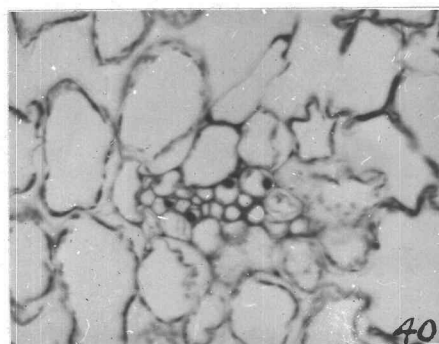
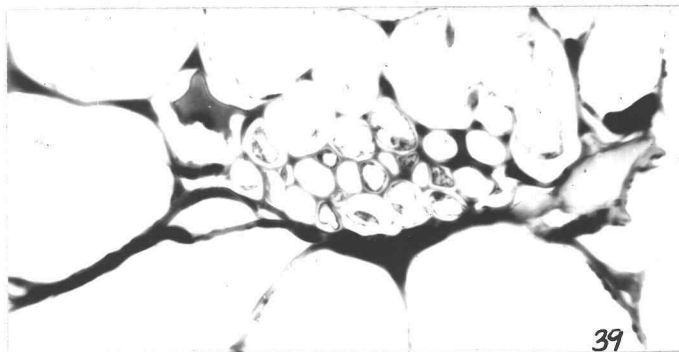


37



38

- Fig. 39. Tulip leaf. CMV. Crushed bundle sheath cells accompanying cell enlargement and cell wall thickening. 400x.
- Fig. 40. Tulip. Healthy leaf same age as Fig. 39. 200x.
- Fig. 41. Tulip leaf. CMV. Cell collapse resulting in wall aggregates interspersed with necrotic protoplasts. 100x.
- Fig. 42. Tulip leaf. CMV. Void formed in mesophyll as result of cell collapse. 100x.
- Fig. 43. Tulip leaf. CMV. Necrosis of a vascular bundle bordering a void. 200x.
- Fig. 44. Tulip leaf. CMV. Vesiculated plastids aggregated about nucleus of mesophyll cell. 800x.
- Fig. 45. Vicia faba leaf. CMV. Necrotic lesion in inoculated leaf covered by collapsed epidermis. 100x.
- Fig. 46. Vicia faba. Healthy leaf same age as Fig. 45. 100x.



- Fig. 47. Vicia faba leaf. CMV. Granular plastids aggregated about nucleus of mesophyll cell (right). 800x.
- Fig. 48. Vicia faba. Healthy leaf. Mesophyll cell from leaf same age as Fig. 47. 800x.
- Fig. 49. Vicia faba leaf. CMV. Vesiculate and diffuse plastids aggregated about nucleus in mesophyll cell. 800x.
- Fig. 50. Vicia faba leaf. CMV. Plastids indistinguishable from finely granular cytoplasm in mesophyll cell. 800x.
- Fig. 51. Vicia faba leaf. CMV. Necrosis of bundle sheath adjacent to xylem of leaf bundle. Exudate in xylem vessels just above the heavily lignified vessels. 400x.
- Fig. 52. Vicia faba stem. CMV. Necrosis of phloem, pericycle parenchyma, and immature pericycle fibers. 200x.

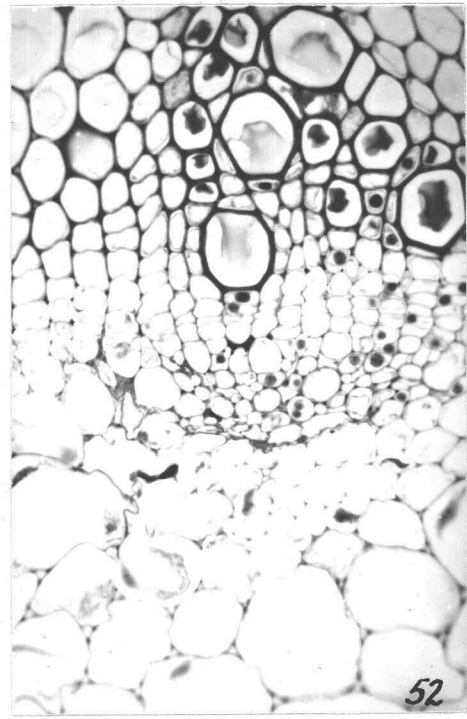
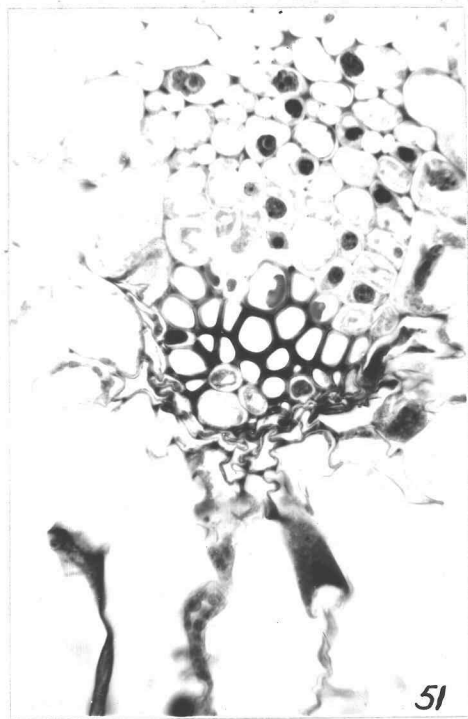
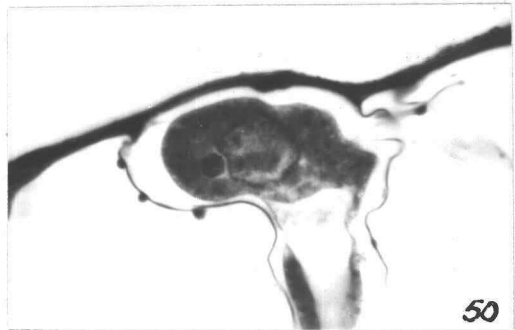
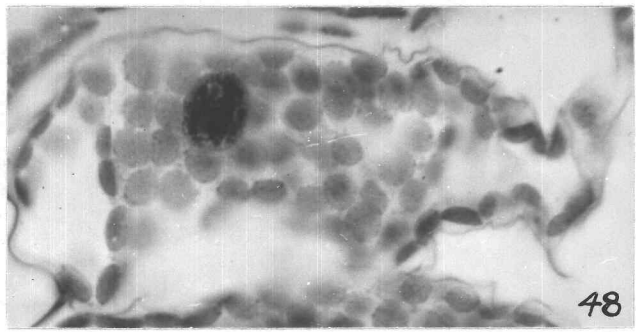
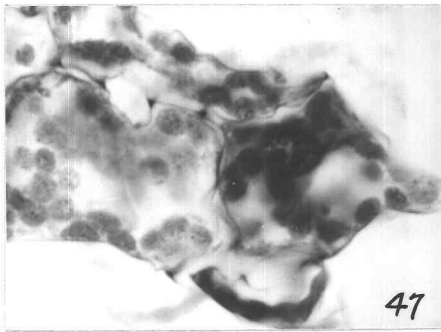


Fig. 53. Vicia faba. Vascular bundle of healthy stem same age as Fig. 52. 200x.

Fig. 54. Vicia faba stem. CMV. Necrosis general throughout vascular bundle and adjacent tissues. 200x.

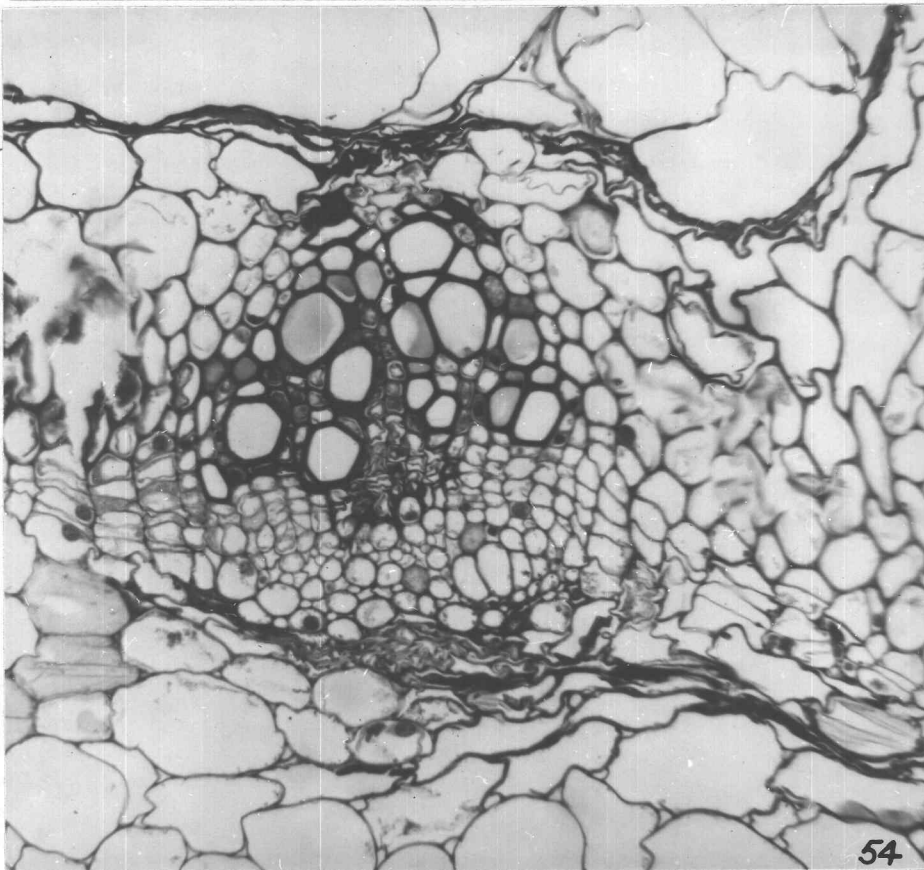
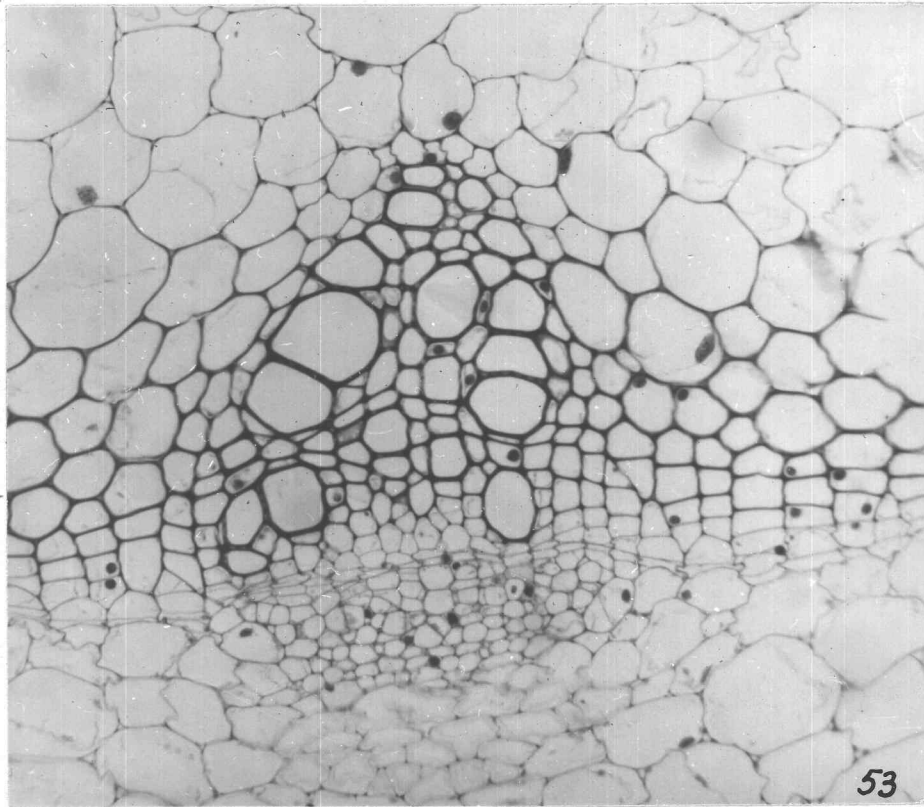


Fig. 55. Vicia faba stem. CMV. Collapsed pericycle parenchyma cells containing necrotic protoplasts. At bottom are immature pericycle fibers with distorted walls. 800x.

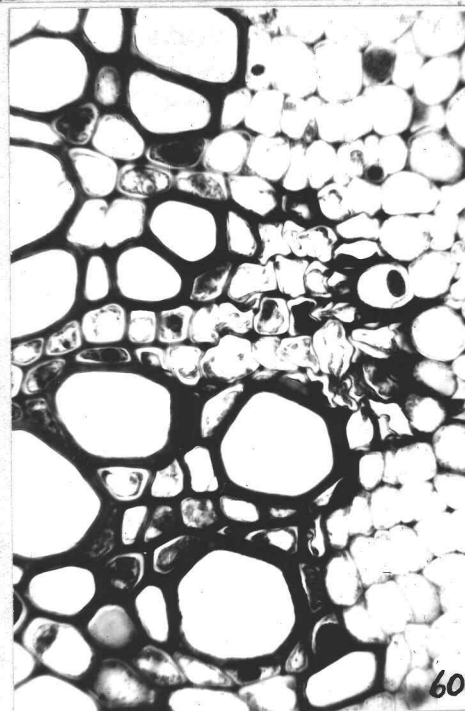
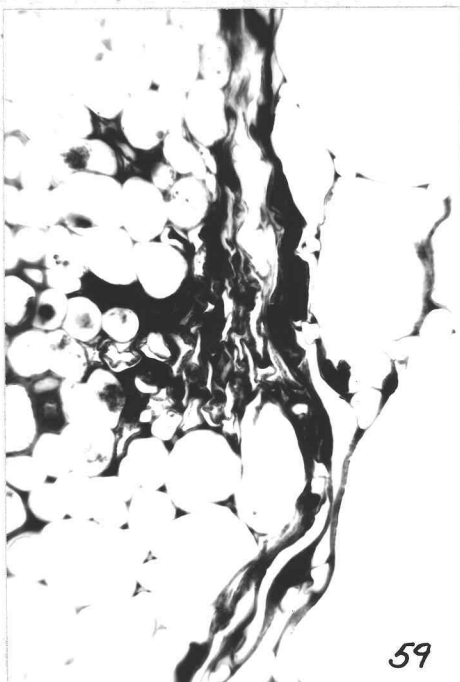
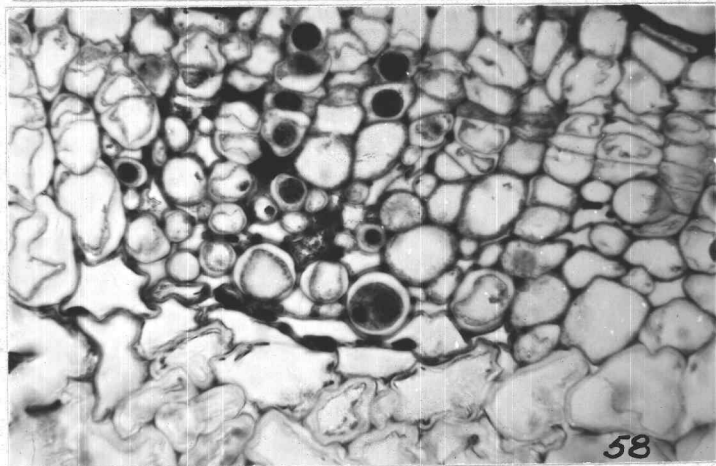
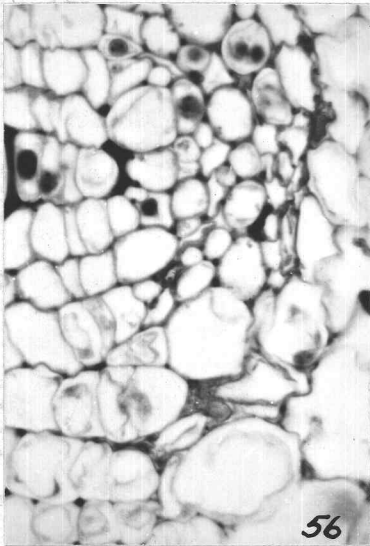
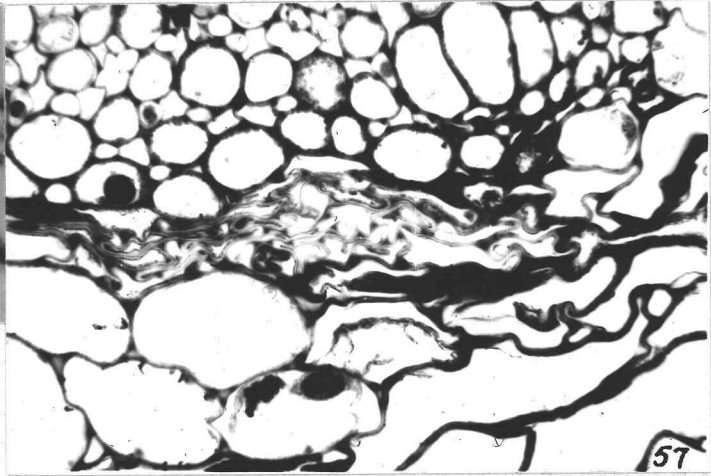
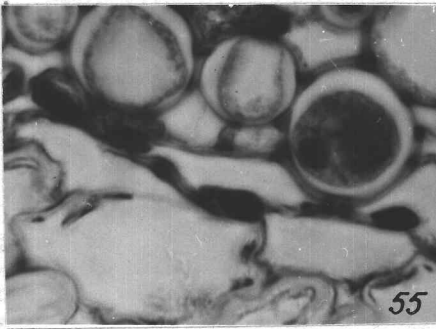
Fig. 56. Vicia faba stem. CMV. Necrosis extending from pericycle parenchyma (upper right) to interfascicular cambium (lower center). 400x.

Fig. 57. Vicia faba stem. CMV. Necrotic and collapsed pericycle fibers (center); necrotic cortical parenchyma (below). 400x.

Fig. 58. Vicia faba stem. CMV. Necrotic phloem (center) and pericycle parenchyma (below). 400x.

Fig. 59. Vicia faba stem. CMV. Mass of necrotic phloem and pericycle parenchyma protoplasts with cell walls forming irregular patterns (center). 400x.

Fig. 60. Vicia faba stem. CMV. Necrotic fascicular cambium (right) and xylem parenchyma (left). 400x.



- Fig. 61. Vicia faba stem. CMV. Finely granular wound gum in large xylem vessel (center) and homogeneous gum in smaller vessel immediately above. 800x.
- Fig. 62. Vicia faba stem. CMV. Necrotic primary xylem resulting from spread of necrosis through pith parenchyma. 100x.
- Fig. 63. Vicia faba stem. CMV. Isolated area of necrotic pith parenchyma (right) adjacent to vascular bundle. 100x.
- Fig. 64. Vicia faba stem. CMV. Spherical bodies in phloem.
Upper left: aggregate of spheres.
Center: single large sphere.
Right center: several small spheres.

